❏   16

Effect of C-terminal truncations on the aggregation propensity of A53E, a familial mutant of α-Synuclein: *An In silico* Study

Airy Sanjeev, Venkata Satish Kumar Mattaparthi[*]
Department of Molecular Biology and Biotechnology,
Tezpur University

ABSTRACT

α-Synuclein, an intrinsically disordered protein, is well known for its role on the onset of Parkinson's Disease (PD), a neurodegenerative disorder. In α-synuclein, several mutations have been known to cause genetic forms of PD. Recently a new familial mutant, A53E of α-synuclein was discovered in a family and found to accelerate the α-synuclein gene, SNCA. But the molecular details about the A53E α-synuclein aggregation were not well studied. It has been recently suggested that two C-terminally truncated α-synuclein (αS C-X): 120 and 123, along with the A53E mutation would cause a more aggressive pathology and an increase in aggregation. So here we demonstrate the effect of C-terminal truncations along with A53E mutation on the aggregation propensity of α-synuclein by comparing the conformational dynamics of A53E full length protein and its C-terminal truncations using molecular dynamics simulation methods. In A53E full length protein we observed stability to be more and also hydrophobic surface (NAC (*non-amyloid β component*) region), number of molecular interactions and interface area between monomeric units to be relatively less than αS C-X. Our findings in this study suggest that more the residues removed from the C-terminal along with A53E mutation have significant effect on the aggregation propensity of α-synuclein.

Corresponding Author:

Venkata Satish Kumar Mattaparthi,
Department of Molecular Biology
and Biotechnology, Tezpur
University, Napaam, Tezpur-7840
28, Assam. Email:
mvenkatasatishkumar@gmail.com

How to Cite:

Airy Sanjeev *et. al.* Effect of C-terminal truncations on the aggregation propensity of A53E, a familial mutant of α-Synuclein: An In silico Study. IJCB. 2018; Volume 7 (Issue 1): Page 16-28.

1. INTRODUCTION

α-Synuclein is a presynaptic and disordered protein, [1] expressed throughout the central nervous system and the main component of Lewy Bodies. Lewy bodies are generally accepted pathological hallmark of Parkinson's disease (PD) [2, 3] that results in toxicity and neuron death [4, 5]. α-Synuclein protein is a product of SNCA, a gene located at position 21 in the long arm of chromosome 4 [6] . Apart from SNCA gene, several other genes are also known for the accumulation of Lewy bodies which are Parkin gene,UCH-L1, PINK1, DJ-1, LRRK2, ATP13A2, and HTRA2 [2,7]. In most of the cases, the familial PD is seen to be carried out with genetic missense mutations of the α-synuclein protein [2]. Among them, A53T, E46K, A30P, H50Q and G51D mutations are well-known. In one of the study, the familial mutants of α-synuclein (A53T and A30P) are observed to be affected by oxidative stress leading to neuronal cell death associated with debilitating PD [8]. It

can also been seen from literature that A53T mutation cause α-synuclein to bind to membrane increasing the toxicity level of the protein whereas A30P localizes the protein in the cytoplasm [9]. Apart from these two major mutants, E46K also binds to the membrane but shows rare impact on toxicity [10] however H50Q does not bind to the membrane very tightly and thereby results in faster aggregation. Now more work has been focused on G51D to check whether it has the same effect as H50Q [11]. Recently A53E, a new mutation which has the tendency to make α-synuclein aggregate faster [12] was identified in a patient at a tender age of 36. But the events leading to the aggregation of A53E α-synuclein are not well understood. However modification and the truncation of the C-terminus of α-synuclein were shown to induce its aggregation. Some of the studies have demonstrated that accumulation of αS C-X is enhanced in neuronal cells as compared with non-neuronal cells. Significantly the expression of familial PD linked mutant α-synuclein is linked with the improved cellular accumulation of αS C-X. In one such study, truncations of α-synuclein, A53E-120 and 123 was created to understand the properties of α-synuclein displaying in yeast that include patterns in localization and toxicity.[13]In the very recent study it has been reported that the C-terminal acidic region (highly charged)may operate as an intra-molecular chaperone by protecting the hydrophobic domain from aggregation [14]. Studies have reported that deletion of amino acids between residues 103-130 results in shortening the C-terminal which probably makes the protein highly hydrophobic and more prone to aggregation. However there are studies that suggested deletion of amino acids from residues 117-122 results in aggregation and adaption of β-sheet configuration [15]. Also it has been mentioned in literature that truncation of amino acid 112 acts as a promoting form for aggregation while truncation of amino acid 126 acts as a protective form [15]. In another recent study it has been stated that truncated (1-120 amino acid) α-synuclein leads to a highly aggregation prone zone in human which is expressed mainly in forebrain areas [16]. It has been noticed that the C-terminal truncation in α-synuclein can lead to the formation of toxic fragments and facilitate α-synuclein oligomerization and propagation [17]. α-Synuclein truncations has the ability to facilitate aggregation of the full-length protein (140 aa) both *in vitro* [18] and *in vivo* [19]. Also it is known that the truncated forms are more prone to oxidative stress than the full-length protein [19]. Hence understanding the effect of A53E mutation in α-synuclein may help us to observe the pathogenesis of PD and its aggregation propensity in a wider view.

To investigate the effect of C-terminal truncation on the aggregation propensity of A53E, we compared the structural dynamics of A53E, truncated A53E-120 and 123using molecular dynamics (MD) simulation. The initial model structure of A53E mutant of α-synuclein was obtained by modifying the experimentally determined NMR structure of α-synuclein (*1XQ8*). The 3D model structure of C-terminal truncated A53E-120 and 123 were obtained from A53E model structure using Pymol. The equilibrated 3D model structure of A53E, truncated A53E-120 and 123 were shown in **Fig. 1**. In A53E full length protein, we noticed stability to be more and hydrophobic surface (NAC (*non-amyloid β component*) region) to be relatively less exposed than αS C-X. Also we observed number of molecular interactions and interface area between monomeric units of A53E full length protein to be lesser in comparison with monomeric units of αS C-X (120 and 123). Hence, we can infer that the aggregation propensity of A53E increases with the truncation of residues in the C-terminal region.
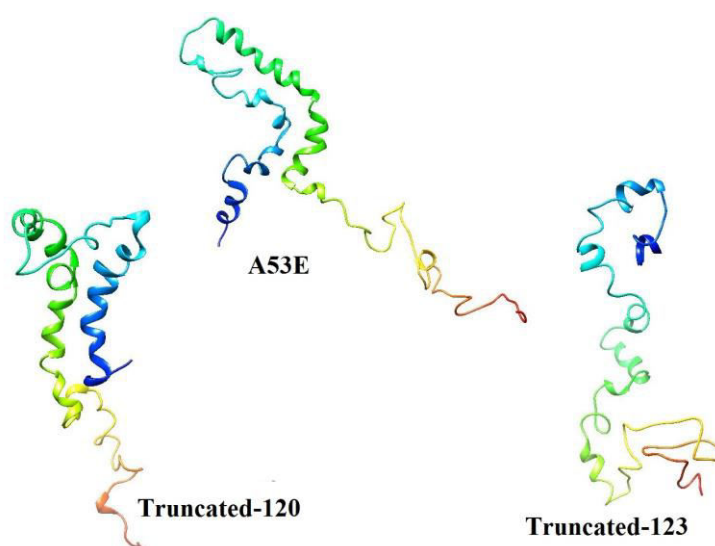
Fig. 1 *Equilibrated structures of the three variants of α-Synuclein (A53E, Truncated-120 and Truncated-123) carried out for a certain interval of time-period using MD simulation*

2.RESEARCH METHOD

2.1. Building of Initial Structures of A53E mutant and its truncated counter-parts (120 and 123):

The model structure of A53E mutant was obtained by modifying the experimentally determined NMR structure of Wild Type (WT) α-synuclein (***PDB ID****: 1XQ8*) taken from Protein Data Bank [20]. Using Swiss-Pdb viewer software, [21] Ala residue at position 53 in the WT structure was replaced with Glu to get the model structure of A53E. The model structure of A53E truncated-120 and 123 were then obtained by removing the residues present in the C-terminal region.

2.2. Simulation Methods:

Using MD module [22] of AMBER 12 software package [23] the simulation study was conducted with PME (Particle Mesh Ewald) of ff99SB-ILDN [24] force field protein parameters on A53E and its two C- terminal truncated-120 and 123 for a time period of 30 ns. The simulation method was carried out using implicit solvation for the initially built structures of the three variants of α-synuclein. It has been reported that using explicit solvation results in errors due to heat capacity variation in water and conformational effects which are resulted from confirmed aqueous volume and therefore we used Generalized Born implicit solvent model [25] to carry out or work. However it is known from literature, [26] that intrinsically disordered protein are highly flexible and can adopt multiple of diverse conformations in the water environment, but using implicit solvation helps to avoid the influence of intermolecular hydrogen bonding interactions and also short and long-range solvent structuring and the effect of local density on the conformations of disordered proteins [26]. The topology and co-ordinate files required were generated using xleap module of AMBER 12 package to run MD simulation. To eradicate the unfavourable contacts, the conformers used for MD simulation were minimized using a total of 500 steps steepest descent followed by 500 steps of conjugate gradient method. Using 2 fs timestep, the obtained minimized conformers were subjected to 100 ps of MD for integration. Systems were then gradually heated up from 0 K to 300 K for a target pressure of 1 atm. Using SHAKE algorithm;[27] bonds to hydrogen atoms were constrained. Particle mesh Ewald (PME) method was used [28, 29] for treating the long-range interactions involved in MD simulations. Subsequently, using Berendsen weak coupling method [30](0.5 ps time constant for heat bath coupling and 0.2 ps pressure relaxation time), MD was performed under constant pressure-temperature conditions (NPT) with temperature regulation. The systems obtained after heating dynamics were then used for equilibration dynamics for a time period of 20 ps. Lastly, NPT MD was carried out for 30 ns using a heat bath coupling time constant of 1ps for the analysis of structural convergence.

2.3. Protein-Protein Interaction Study:

To study the interactions between the monomeric units present in the dimers of A53E and truncated-120 and 123, we constructed the corresponding dimers using the respective equilibrated structures. For obtaining the dimer conformers, we have used PatchDock server, [31] a molecular docking tool which generates rigid docking model of dimers of A53E and truncated A53E-120 and 123. The PatchDock is an online docking server which operates by computing the 3D transformations of one of the given monomer molecule out of two molecules with respect to the other one. The main objective of the server is to maximize the surface shape complementarity score and minimize the number of steric clashes. The server is based on geometry docking algorithm [31] that finds optimum candidate solutions and uses RMSD (Root Mean Square Deviation) clustering to remove redundant candidate solutions. Thereby, each solution was given a particular score according to geometric fit and atomic desolvation energy [32]. In our study the RMSD value was taken as 4 Å for clustering solutions. To obtain the protein-protein interactions between the monomeric units of dimer of A53E mutant and its truncated counterparts-A53E-120 and 123 we used PDBSum online server [33]. The server gives a detail about the interacting interface, interfaces between the chains, overview of which chains interact with the other chain and the interactions across any selected interface of the dimer complex. The best conformer obtained from PatchDock based on geometric surface area, surface shape complementarity score, atomic contact energy (ACE) was submitted onto the PDBSum server. The summary of the bonded, non-bonded contacts and the interacting residues involved between the monomeric units in the dimer were obtained from PDBSum.

In the similar way, we have also studied protein-protein interactions for hetero-dimers: **a)** (A53E full protein)-(C-terminal truncated), **b)** (A53E full protein)-(truncated-120) and **c)** (A53E full protein)-(truncated-123) using PDBSum online server.

2.4. Analysis of trajectory:

Structural analysis of A53E and truncated-120 and 123were carried out using their respective MD simulation trajectory files. To determine the structural properties (Root Mean Square Deviation (RMSD), Atomic Fluctuation (RMSF), Radius of Gyration (Rg), Solvent Accessible Surface Area (SASA), secondary structure development) cpptraj module [34] of AMBER package was used. We used various softwares such as UCSF Chimera [35], VMD [36], Swiss-pdb viewer and YASARA [37] for inspecting 3D structure of the molecule. For generating graphs for the structures, xmgrace plotting tool was used.

2.5. Entropy Calculation:

We measured the entropy of A53E mutant and the truncated-120 and truncated-123. The conformational entropy for A53E mutant and the truncated ones were calculated using gas phase statistical mechanics. This involves principal component analysis (quasi-harmonic approximation) that provides the first decomposition of correlation in particle motion [38]. Thus the entropy is calculated analytically as a sum of independent quantum harmonic oscillators.

3. RESULTS AND ANALYSIS

To study the effect of C-terminal truncations on the aggregation propensity of A53E mutant of α-synuclein, we have investigated the conformational dynamics of A53Emutant and its truncated counter-partsA53E-120 and 123 using all atom molecular dynamics (MD) simulation.

3.1. Root Mean Square Deviation (RMSD) Analysis:

For measuring the C-α root mean square deviation, the degree of conformational changes in A53E and truncated-120 and 123 during the time course of simulation was monitored. The backbone RMSD values for the structures of three variants relative to their corresponding initial structure have been calculated and represented in **Fig. 2.**

We observed the RMSD profile in the case of A53E protein to be completely different from its two truncated counterparts, 120 and 123.In A53E, the RMSD values settles around35 Å after 18 ns while in the truncated versions of A53E, 120 and 123, we observed the RMSD value settles around 25 Å after 10 ns. From the RMSD plots it can be observed that conformational changes in A53E are more than the truncated versions of A53E. This is mainly due to the presence of flexible loops and coils in the C-terminal region of A53E.
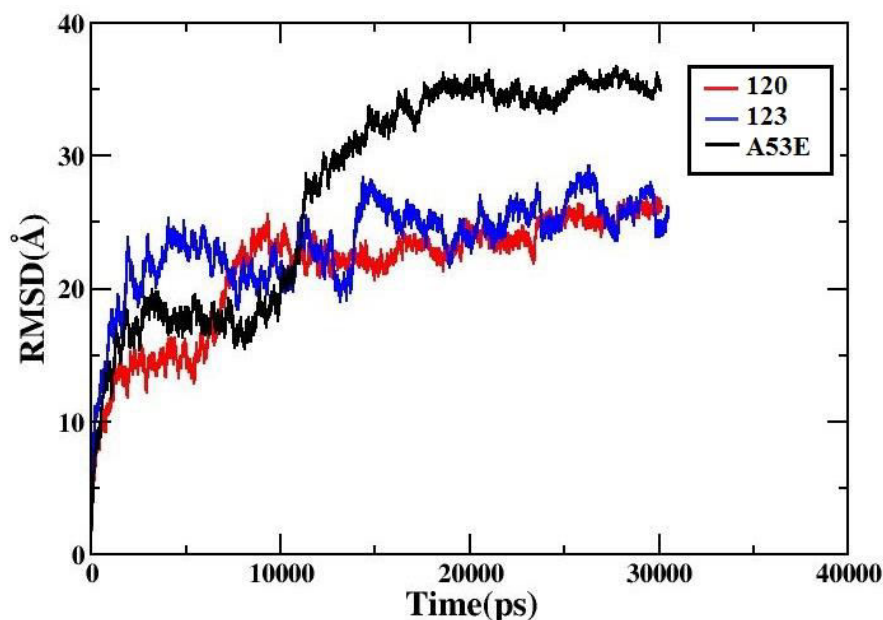
Fig. 2 *RMSD (Root Mean Square Deviation) as a function of simulation time for the A53E protein shown in black, truncated-120 in red and truncated-123 in blue color*

The degree of conformational changes in A53E mutant and its two truncated counter-parts (truncated-120 and truncated-123) can be seen from the snapshots taken at different intervals of the simulation time

period as shown in **Fig. 3**. From **Fig. 3**, we noticed helical contents in A53E mutant to be higher when compared to its truncated counter-parts-120 and 123. Hence we see αS C-X to undergo aggregation more readily than A53E mutant of α-synuclein [13]. Thus we can infer as more number of amino acids are removed from the C-terminal region of α-synuclein, the aggregation propensity will increase as seen from earlier literature [13].
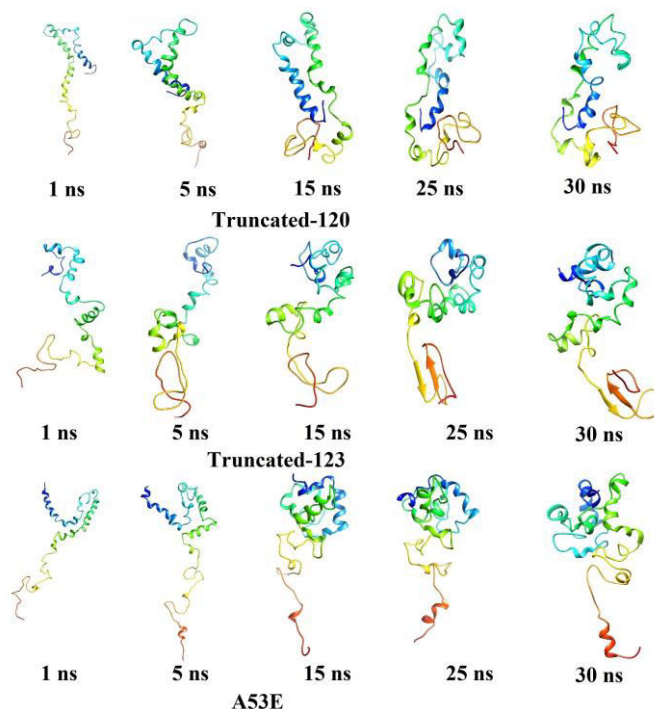
Fig. 3 *Snapshots of the A53E mutant, truncated-120 and truncated-123 for a time-period of 30 ns. Different flexible folding conformations of A53E and the two truncated versions can be seen at various stages of simulation period*

We also checked the stability of the A53E and its truncated counter-parts by analyzing the total, kinetic and potential energy (**Fig. 4**). From the potential energy profile we see A53E mutant and also the truncated counter-parts: 120 and 123 to be stable. We noticed A53E (-2200 kcal/mol) mutant to be relatively more stable than its truncated counter-parts 120 (-1600 kcal/mol) and 123 (-1800 kcal/mol). This indicates the presence of disorderness in αS C-X structures.
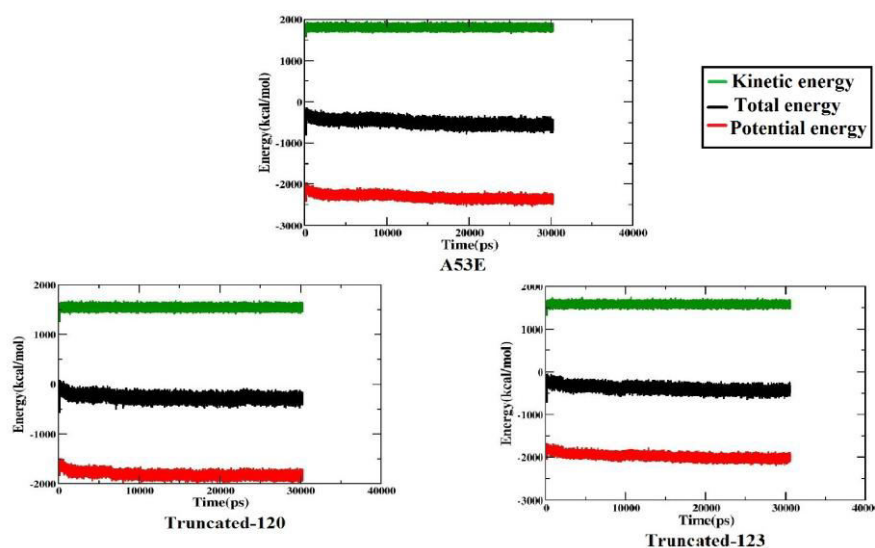

Fig. 4 *Energy as a function of simulation time for the A53E protein, truncated-120 and truncated-123*

3.2. B-Factor and RMSF Analysis:

The B factor and root mean square fluctuation (RMSF) of C-α atom with respect to the residue index were analyzed to check the local deformability in A53E mutant and truncated-120 and 123. B-factor and RMSF values are related to one another. Root mean-square fluctuations (RMSF) give information about the thermal stability, local structural flexibility and heterogeneity of macromolecules, whereas B-factors represent spatial fluctuations of atoms around their equilibrium position. The motion is well-defined as an isotropic Gaussian distribution of displacements about the average position. The B factor and RMSF values obtained for the backbone C-α atom in all the three cases were calculated from MD simulation trajectory and were plotted against their residue index (**Fig. 5A & B**).

RMSF showed that some fluctuations occurred in the C-terminal loop regions of A53E with one high peak at around 20 Å and other residues are stable with less fluctuation. The RMSF plot also confirms that the fluctuations of the residues are more prominent in the C-terminal region of A53E and less in the other regions of the protein. From these plots we can see the flexible regions are higher in case of A53E than truncated-120 and 123. The C-terminal region of α-synuclein is highly negatively charged. This is due to the truncation of residues present in the flexible C-terminal region of α-synuclein, the aggregation propensity increases. In the case of truncated-123, we see C-α atom of the residues in the NAC region shows more flexibility than the other residues. NAC region of α-synuclein are known for their differing flexibility in different conditions [39]. Since the NAC region is considered to be important for the aggregation propensity [40] we expect A53E truncated counter-parts may undergo aggregation faster than A53E mutant itself.
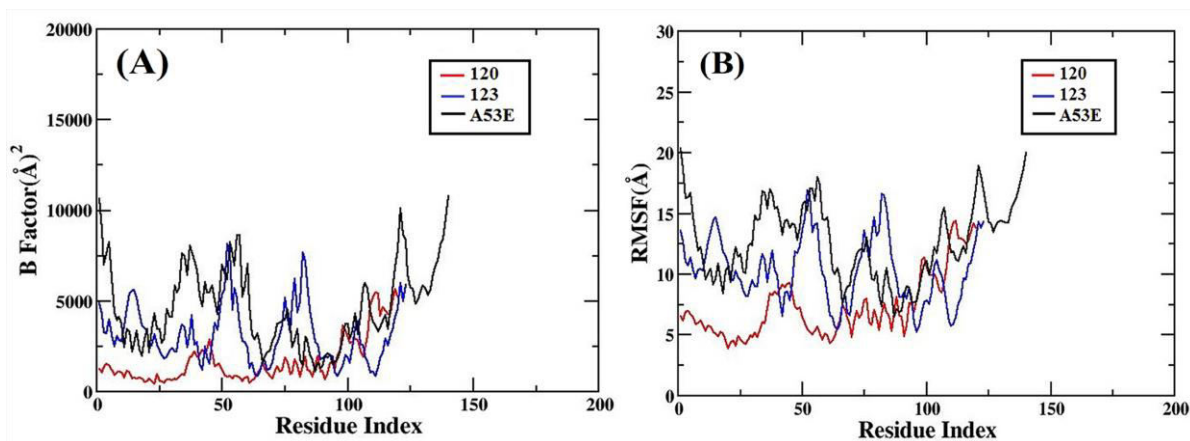

Fig. 5 *A) B factor analysis as a function of residue index for the A53E protein, truncated-120 and truncated-123 B) RMSF (Root Mean Square Fluctuation) as a function of residue index for the A53E protein, truncated-120 and truncated-123*

3.3. Radius of Gyration (Rg) analysis:

To check the compactness and level of extension for the conformers of A53E and its counter-parts truncated-120 and truncated-123, we performed Rg analysis (**Fig. 6A**). From the Rg plots, we can see A53E truncated counter-parts show higher degree of compactness whileA53E mutant shows less degree of compactness. The presence of flexible regions in the C-terminal and strong intra-molecular interactions between the residues in N and C-terminals in case of A53E lowers the degree of compactness when compared to the truncater-120 and 123.

We also calculated radius of gyration exclusively for the NAC region which is depicted in **Fig. 6B**. From **Fig. 6B**, we observed truncated-120 to have higher radius of gyration value for the NAC region than the other two variants, truncated-123 and A53E. We can thus infer that C-terminal truncation in α synuclein has a significant effect on the structure near the NAC region (*fibril forming core*), known for its aggregation propensity.
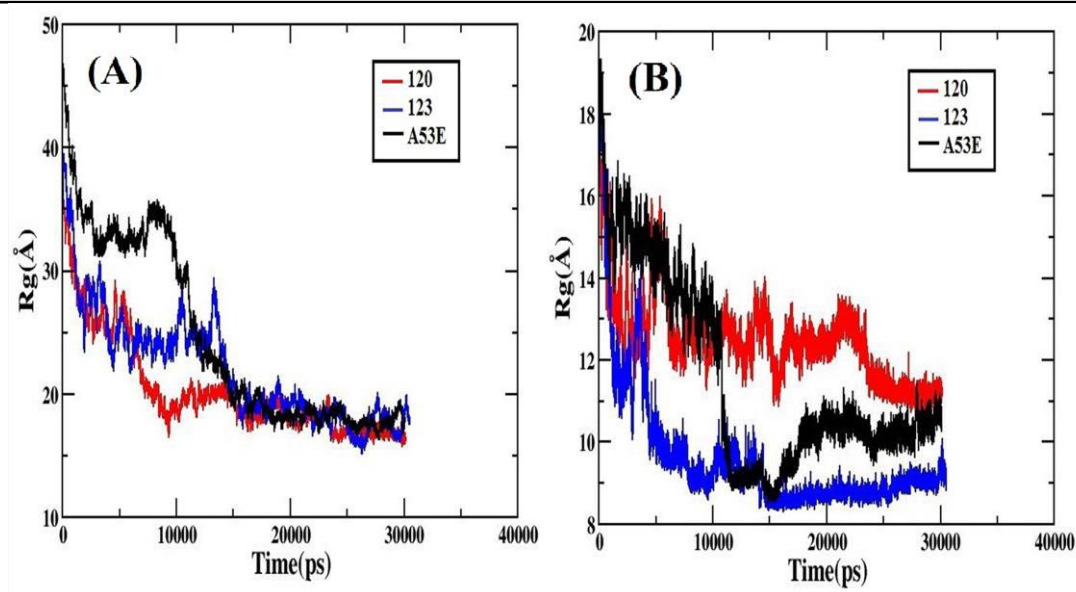
Fig. 6 A) *Rg (Radius of Gyration) for the entire protein A53E, truncated-120 and 123 as a function of simulation time* **B)** *Rg (Radius of Gyration) for the NAC (non-amyloid β-component) region alone for A53E, truncated-120 and 123 as a function of simulation time*

3.4. Solvent Accessible Surface Area (SASA) Analysis:

To check the regions exposed to the solvent surface area and the finer details on the solvent accessible region in A53E and its two truncated counter-parts we calculated SASA for the entire region of the protein (**Fig. 7A & B**) as well as exclusively for the NAC region (**Fig. 8**). SASA results shows that in the case of truncated A53E the accessibility was retained with less changes during the time course of simulation and confirmed that the residues present were well exposed to the solvent. We have also calculated the fraction of Polar and Non-polar regions for the three variants of α-synuclein. The percentage of polar and non-polar regions along with the solvent accessible surface area for the total region as well as for the NAC domain in the three variants can be seen in **Table 1 & 2**. From **Table 2**, it can be seen that the solvent accessible surface area for truncated-120 is highest for the NAC region, the fibril core domain of α-synuclein. We can thus infer that the aggregation propensity favours for the truncated counter-parts of A53E as proposed in earlier literature.
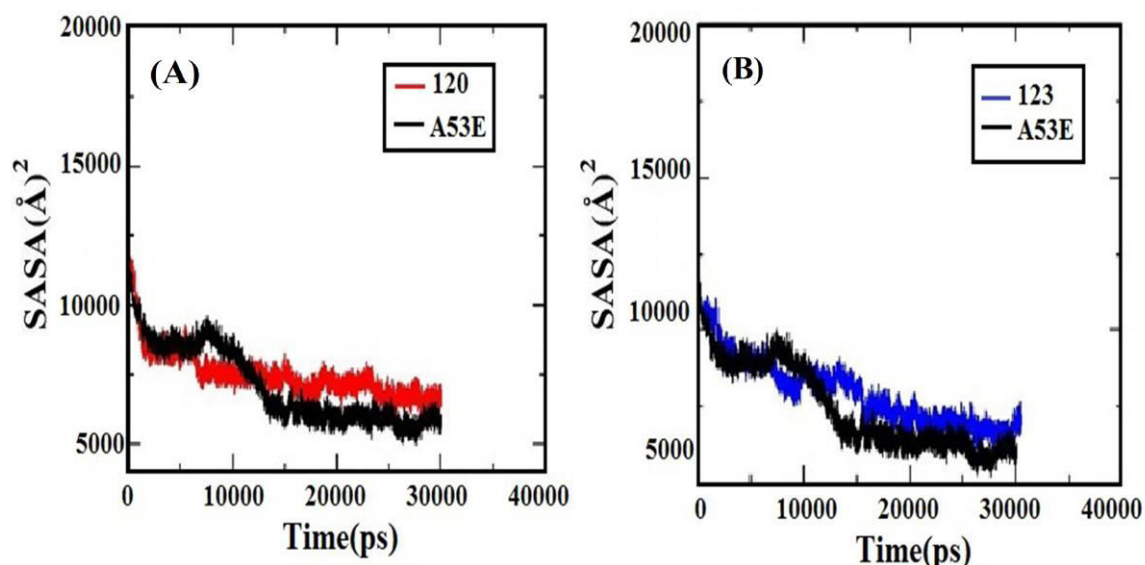
Fig. 7 A) *SASA (Solvent Accessible Surface Area) for the entire protein A53E, truncated-120 and* **B)** *SASA (Solvent Accessible Surface Area) for the entire protein A53E and truncated-123 as a function of simulation time*
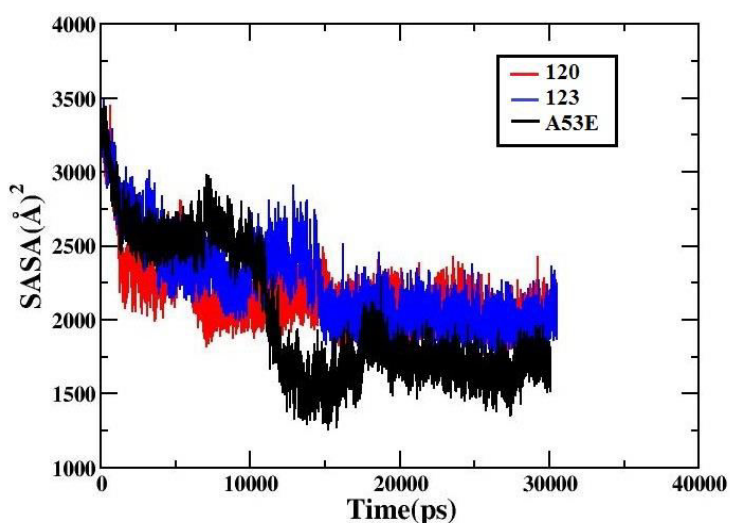
Table 1. Solvent Accessible Surface Area analysis (SASA) and Molecular Surface Area (MSA) Analysis which depicts the total area, polar area and non-polar area of A53E and its counterparts showing the most hydrophobic interactions of the A53E protein than the corresponding mutants

α-Synuclein Variants	Solvent Accessible Surface Area($\mathring{A}$)^2			Molecular Surface Area($\mathring{A}$)^2		
	Total Area	Polar Area	Non-Polar Area	Total Area	Polar Area	Non-Polar Area
A53E	10446.01	6265.57	4180.43	8409.08	3839.32	4569.76
120	8711.39	5231.98	3479.41	7203.10	3347.31	3855.79
123	9012.08	5665.66	3346.43	7024.83	3313.05	3711.78

Table 2: Solvent Accessible Surface Area analysis for the NAC region (61-95) of A53E showing the most hydrophobic interactions of the A53E protein than the corresponding mutants.

α-Synuclein Variants	Solvent Accessible Surface Area($\acute{A}$)^2
A53E	1669.061
120	1912.607
123	1832.82

In **Fig. 8**, we calculated the SASA exclusively for the NAC region (61-95) for the three variants of α-synuclein (A53E, A53E truncated-120 and 123).From the figure, we observed the value of SASA in the case of A53E to be less than its two counterparts, truncated-120 and truncated-123. Among the three variants, we see truncated-120 to have the highest solvent accessible surface area. Thus, from SASA plot (**Fig. 8**) and **Table 1 & 2,** we noticed A53E mutant to have SASA and Molecular Surface Area (MSA) lesser than its other two truncated counter-parts. As NAC region is the main fibril core region for α-synuclein, [39] the enhanced hydrophobic exposure for the two truncated counter-parts of A53E actually leads to higher aggregation propensity.

**Fig. 8** *SASA (Solvent Accessible Surface Area) for the NAC (non-amyloid β component) region alone for A53E, truncated-120 and truncated-123 as a function of simulation time*

3.5. Secondary Structure analysis:

Using the Kabsch and Sander algorithm, the secondary structure analysis was carried out for A53E mutant and its two truncated counter-parts (truncated-120 and truncated-123) of α-synuclein, which were incorporated in their DSSP (**D**ictionary of **S**econdary **S**tructure for **P**rotein) program [41]. The results were plotted in **Fig. 9**.

The plot shows the secondary structural variation of each residue as a function of simulation time period. In the case of A53E mutant, we observed loops in the C-terminal region show more flexibility with α-helix, 3_{10} helix, β bridge and turn occurrence. In addition, we also see anti-parallel β sheets near the C-terminal regions (residue index: 97-100, 118-120) and in the other regions, we observed secondary structure transitions from 3_{10} helix and α-helix to turns. In case of truncated-120 and 123; we observed some residues in the C-terminal and NAC region to have anti-parallel β sheets (residue index: 98-100,105 in the case of truncated-120; 91-93,100-102, 121 in truncated-123). In addition to that, we observed parallel β sheets in the NAC region (residue index: 80, 94-95) for truncated-123. While in the other regions of variants, we observed many of the residues showing secondary structure transitions from helix to turns. Thus from these observations, we can conclude that truncated counter-parts of A53E have more amount of β-strands in the NAC region when compared to A53E mutant.
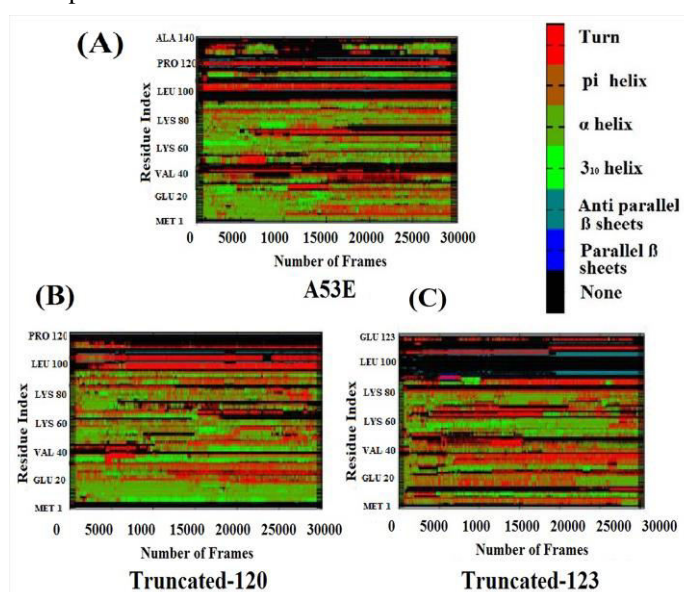
Fig. 9 *Secondary Structure Analysis for **A**) A53E protein, **B**) truncated-120 and **C**)truncated-123 using DSSP (Dictionary of Secondary Structure of Protein) as a function of number of frames*

We also calculated the percentage of individual secondary structure contents in the three variants across all conformations that were sampled during the production run of simulation study and the results were summarized in **Table 3.** We also quantified the probable secondary structures that each residue can adopt in the case of three variants of α-synuclein (**see Fig. S1**). From ***Fig. S1,*** we noticed the various secondary structure contents that are present in A53E, A53E truncated-120 and truncated-123 as a function of residue index. We observed truncated-123 to have a higher amount β sheets than the corresponding counterparts. Our results support the hypothesis proposed earlier which suggests that truncated counter-parts of A53E can aggregate faster than A53E itself.

Table 3. Secondary Structure content of the A53E, truncated-120 and 123 of α-synuclein showing the secondary contents of α- helix, β-sheets, Turns, 3_{10}–helix, π helix and Coils

α-Synuclein Variants	Secondary Structure content					
	α- helix (%)	β-sheets (%)	Turns (%)	3_{10} -helix (%)	Coils (%)	π helix (%)
A53E	20.7	23.6	41.4	0.0	14.3	0.0
120	34.2	2.5	15.0	14.2	34.2	0.0
123	13.8	10.6	39.0	3.3	33.3	0.0

We also calculated the conformational entropy for A53E mutant and its truncated counter-parts: 120 and 123 from the analysis trajectory file. The details for the conformational entropy for the three variants are summarized in **Table 4**. From *Table 4*, we observed the entropy value for truncated-120 (1780.220 cal/mol-K) is least when compared to truncated 123 (1896.393 cal/mol-K) and A53E mutant (2168.453 cal/mol-K). Thus we can suggest that truncating the C-terminal residues do have an impact on the entropy and also on the aggregation propensity.

Table 4. *Summary of the entropy calculation for A53E mutant, truncated-120 and 123 of α-synuclein*

α-Synuclein Variants	Conformational Entropy (cal/mol-K)
A53E	*2168.453*
120	*1780.220*
123	*1896.393*

3.6. Protein-Protein Interaction Study for homo-dimer and hetero-dimer:

Molecular interactions between homo-dimer of A53E and αS C-X (120 and 123):

We also studied protein-protein interactions between the monomeric units of the dimers of A53E and truncated-120 and 123 using PDBSum server [33]. The protein-protein interactions in the dimers play an essential step in understanding the aggregation process because they may represent the building blocks for large oligomers. The atomic knowledge of the dimers of A53E and truncated A53E were obtained using PatchDock online server. This server gives a detail about various candidate solutions based on geometric shape complementarity score, atomic contact energy (ACE) and geometric surface area. Patch Dock results for the three variants of α-synuclein were summarized in **Table S1.** The details about the geometric shape complementarity score, approximate interface area and atomic contact energy (ACE) are depicted in the **Table S1**. From *Table S1*, it was observed that the interface area for truncated-120 and truncated-123 were higher when compared withA53E full protein. The interface area for truncated-120 and 123 were 2291.20 and 2728.10 Å^2 respectively. This suggests that the truncated counter-parts of A53E have more tendencies to form dimer, oligomer and thus aggregate faster than the A53E full protein.

To investigate the residues involved in protein-protein interaction, the conformer having the best ACE value obtained from PatchDock server, (see **Fig. S2**) was chosen and submitted onto PDBSum server. The details of the interface area, which chains interact with other chain, interactions across any selected interface and which residues actually interact across that interface were predicted by PDBSum. Here the interface residues of a protein are defined as those residues whose contact distances from the interacting protein partner are less than 6 Å. These interfaces across the complexes were found to be stabilized by molecular interactions such as hydrogen bonds, salt-bridge, disulphide bonds and non-bonded contacts (see **Fig. S3**). The details of the interface plot statistics for the dimers of the three variants of α-synuclein are summarized in **Table S2**. From *Table S2*; we observe the total number of non-bonded contacts for the truncated versions of A53E to be more than the A53E full protein. Thus from our observations, we can see that the aggregation propensity to be higher in the truncated versions of A53E than A53E full protein.

Molecular interactions between hetero-dimer of A53E full protein and the truncated versions:

It has been reported in recent literature that αS C-X is enriched in the pathological α-synuclein aggregates. And also accumulation of αS C-X is enhanced in neuronal cells when compared with non-neuronal cells. So we investigated the protein-protein interactions between the C-terminally truncated versions and A53E full protein. The largest ACE conformer obtained from PatchDock server, (see **Fig. S4**) was chosen for protein-protein interaction study. The interactions between the monomeric units in the heterodimer of **a)** (A53E full protein) - (C-terminally truncated), **b)** (A53E full protein) - (truncated-120) and **c)** (A53E full protein) - (truncated-123) were analyzed using PDBSum online server. The number of molecular interactions (hydrogen bonds, salt-bridge, disulphide bonds and non-bonded contacts), the interacting residues and the interface area determined in the three hetero-dimer complexes were depicted in **Fig. S5** and summarized in the **Table S3**. From *Table S3*, it is observed that the number of interface residues, interface area and number of hydrogen bonds for (A53E full protein) - (truncated-120) was more when compared to the hetero-dimer of (A53E full protein) - (C-terminally truncated) and (A53E full protein) - (truncated-123). Thus we can infer that more the C-terminal truncation more will be its association with α-

synuclein full length protein. This is so because the C-terminal truncation makes the protein highly hydrophobic and more prone to aggregation.

4. Conclusions

In this work, we investigate the effect of C-terminal truncations along with A53E mutation, a familial mutant on the aggregation propensity of α-synuclein by comparing the conformational dynamics of A53E full length protein and its C-terminal truncations. We observed the structural features of A53E mutant along with the C-terminal truncation to induce relatively more aggregation prone structure than the well-studied wild type of α-synuclein. We also noticed A53E-120 truncation to show aggregation more than A53E-123 truncation. Thus by removing amino acid residues from the C-terminal region, accumulation of α-synuclein increases and also its aggregation propensity. Between the two truncated counterparts of A53E, we noticed higher number of N- and C-terminal contacts in A53E-120 rather than A53E-123 which supports our hypothesis that A53E-120 can aggregate at a faster rate. In the truncated A53E protein, we see the NAC region is highly exposed than the A53E full protein. We also studied the interaction between A53E full length protein and its C-terminal truncated versions and found more the C-terminal truncation more will be its association with α-synuclein full length protein. So we report here that more the residues removed from the C-terminal along with A53E mutation have significant effect on the aggregation propensity of α-synuclein.

REFERENCES

[1] Uversky, V.N. A protein-chameleon: conformational plasticity of alpha-synuclein, a disordered protein involved in neurodegenerative disorders. *Journal of Biomolecular Structure and Dynamics*, 2003, 21, 211-234. Doi: 10.1080/07391102.2003.10506918

[2] Polymeropoulos, M.H.; Lavedan, C.; Leroy, E.; Ide, S.E.; Dehejia, A.; Dutra, A.; Pike, B.; Root, H.; Rubenstein, J.; Boyer, R.; Stenroos, E.S.; Chandrasekharappa, S.; Athanassiadou, A.; Papapetropoulos, T.; Johnson, W.G.; Lazzarini, A.M.; Duvoisin, R.C.; Di Iorio, G.; Golbe, L.I.; Nussbaum, R.L. Mutation in the alpha-synuclein gene identified in families with Parkinson's disease. *Science*, 1997, 276, 2045-2047. Doi: 10.1126/science.276.5321.2045

[3] Spillantini, M.G.; Schmidt, M.L.; Lee, V.M.; Trojanowski, J.Q.; Jakes, R.; Goedert, M. Alpha-synuclein in Lewy bodies. *Nature*, 1997, 388, 839-840. Doi: 10.1038/42166

[4] Jin, H.; Kanthasamy, A.; Ghosh, A.; Yang, Y.; Anantharam, V.; Kanthasamy, A.G. α-Synuclein negatively regulates protein kinase Cδ expression to suppress apoptosis in dopaminergic neurons by reducing p300 histone acetyltransferase activity. *Journal of Neuroscience*, 2011, 31, 2035-2051. Doi: 10.1523/jneurosci.5634-10.2011

[5] Petrucelli, L.; Dickson, D.W. *Neuropathology of Parkinson's disease: Molecular and Therapeutic Insights from Model Systems*, 2008, 35-48, New York, NY: *Elsevier* Inc. Doi: 10.1016/b978-0-12-374028-1.00003-8

[6] Shibasaki, Y.; Baillie, D.A.; St Clair, D.; Brookes, A.J. High resolution mapping of SNCA encoding alpha-synuclein, the non-A beta component of Alzheimer's disease amyloid precursor, to human chromosome 4q21.3–>q22 by fluorescence in situ hybridization. *Cytogenetics and Cell Genetics*, 1995, 71, 54–55. Doi: 10.1159/000134061

[7] Ross, O.A.; Braithwaite, A.T.; Farrer, M.J. *Genetics of Parkinson's disease. Parkinson's disease: Molecular and Therapeutic Insights from Model Systems*, 2008, *9-25*, New York, NY: *Elsevier* Inc. Doi: 10.1016/b978-0-12-374028-1.00002-6

[8] Kanda, S.; Bishop, J.F.; Eglitis, M.A.; Yang, Y.; Mouradian, M.M. Enhanced vulnerability to oxidative stress by alpha-synuclein mutations and C-terminal truncation. *Neuroscience*, 2000, 97, 279-284. Doi: 10.1016/s0306-4522(00)00077-4

[9] Sharma, N.; Brandis, K.A.; Herrera, S.K.; Johnson, B.E.; Vaidya, T.; Shrestha, R.; Debburman, S.K. Alpha-Synuclein budding yeast model: toxicity enhanced by impaired proteasome and

oxidative stress. *Journal of Molecular Neuroscience*, 2006, 28, 161-178. Doi: 10.1385/jmn:28:2:161

[10] Volles, M.J.; Lansbury, P.T. Jr Relationships between the sequence of alpha-synuclein and its membrane affinity, fibrillization propensity, and yeast toxicity. *Journal of Molecular Biology*, 2007, 366, 1510-1522. Doi: 10.1016/j.jmb.2006.12.044

[11] Ghosh, D.; Mondal, M.; Mohite, G.M.; Singh, P.K.; Ranjan, P.; Anoop, A.; Ghosh, S.; Jha, N.N.; Kumar, A.; Maji, S.K. The Parkinson's disease-associated H50Q mutation accelerates α-Synuclein aggregation in vitro. *Biochemistry*, 2013, 52, 6925-6927. Doi: 10.1021/bi400999d

[12] Pasanen, P.; Myllykangas, L.; Siitonen, M.; Raunio, A.; Kaakkola, S.; Lyytinen, J.; Tienari, P.J.; Poyhonen, M.; Paetau, A. Novel α-synuclein mutation A53E associated with a typical multiple system atrophy and Parkinson's disease-type pathology. *Neurobiology of Aging,* 2014, 35, 2180.e1-5. Doi: 10.1016/j.neurobiolaging.2014.03.024

[13] Dunn, A.; Graham, L. Creation of Novel alpha-Synuclein Mutation A53E Truncations 123 and 120 for Future Study in Budding Yeast. Lake Forest College*: Eukaryon*, 2015, 11.

[14] Park, S.; Yoon, J.; Jang, S.; Lee, K.; Shin, S. The role of the acidic domain of α-synuclein in amyloid fibril formation: a molecular dynamics study. *Journal of Biomolecular Structure and Dynamics,* 2015, 34, 376-383. Doi: 10.1080/07391102.2015.1033016

[15] **Kukulka, N.** Uncovering the Mysteries of Alpha-Synuclein Natural Truncation Variants. Lake Forest College: *Eukaryon*, 2013, 9.

[16] Hall, K.; Yang, S.; Sauchanka, O.; Spillantini, M.G.; Anichtchik, O. Behavioral deficits in transgenic mice expressing human truncated (1–120 amino acid) alpha-synuclein. *Experimental Neurology*, 2015, 264, 8–13. Doi: 10.1016/j.expneurol.2014.11.003

[17] Games, D.; Valera, E.; Spencer, B.; Rockenstein, E.; Mante, M.; Adame, A.; Patrick, C.; Ubhi, K.; Nuber, S.; Sacayon, P.; Zago, W.; Seubert, P.; Barbour, R.; Schenk, D.; Masliah, E. Reducing C-Terminal-Truncated Alpha-Synuclein by Immunotherapy Attenuates Neurodegeneration and Propagation in Parkinson's Disease-Like Models. *Journal of Neuroscience*, 2014, 34, 9441–9454. Doi: 10.1523/jneurosci.5314-13.2014

[18] Liu, C.W.; Giasson, B.I.; Lewis, K.A.; Lee, V.M.; DeMartino, G.N.; Thomas, P.J. A precipitating role for truncated alpha-synuclein and the proteasome in alpha-synuclein aggregation: Implications for pathogenesis of Parkinson disease. *Journal of Biological Chemistry*, 2005, 280, 22670- 22678. Doi: 10.1074/jbc.m501508200

[19] Ulusoy, A.; Febbraro, F.; Jensen, P.H.; Kirik, D.; Romero-Ramos, M. Co-expression of C-terminal truncated alpha-synuclein enhances full-length alpha- synuclein-induced pathology. *European Journal of Neuroscience*, 2010, 32, 409-422. Doi: 10.1111/j.1460-9568.2010.07284.x

[20] Berman, H.M.; Westbrook, J.; Feng, Z.; Gilliland, G.; Bhat, T.N.; Weissig, H.; Shindyalov, I.N.; Bourne, P.E. The protein data bank. *Nucleic Acids Research*, 2000, 28, 235-242. Doi: 10.1093/nar/28.1.235

[21] Guex, N.; Peitsch, M.C. SWISS-MODEL and the Swiss-pdb viewer: an environment for comparative protein modeling. *Electrophoresis*, 1997, 18, 2714-2723. Doi: 10.1002/elps.1150181505

[22] Kaus, J.W.; Pierce, L.T.; Walker, R.C.; McCammon, J.A. Improving the Efficiency of Free Energy Calculations in the Amber Molecular Dynamics Package. *Journal of Chemical Theory and Computation*, 2012, 9: 4131-4139. Doi: 10.1021/ct400340s

[23] Pearlman, D.A.; Case, D.A.; Caldwell, J.W.; Ross, W.S.; Cheatham, III T.E.; DeBolt, S.; Ferguson, D.; Seibel, G.; Kollman, P. AMBER, a package of computer programs for applying molecular mechanics, normal mode analysis, molecular dynamics and free energy calculations to simulate the structural and energetic properties of molecules. *Computer Physics Communications*, 1995, 91: 1-41. Doi: 10.1016/0010-4655(95)00041-d

[24] Henriques, J.; Cragnell, C.; Skepo, M. Molecular Dynamics Simulations of Intrinsically Disordered Proteins: Force Field Evaluation and Comparison with Experiment. *Journal of Chemical Theory and Computation*, 2015, 11, 3420. Doi: 10.1021/ct501178z

[25] Onufriev, A.; Bashford, D.; Case, D.A. Exploring protein native states and large-scale conformational changes with a modified generalized born model. *Proteins,* 2004, 55: 383. Doi: 10.1002/prot.20033

[26] Coskuner, O.; Wise-Scira, O. Structures and Free Energy Landscapes of the A53T Mutant-Type α-Synuclein Protein and Impact of A53T Mutation on the Structures of the Wild-Type α-Synuclein Protein with Dynamics. *ACS Chemical Neuroscience*, 2013, 4, 1101−1113. Doi: 10.1021/cn400041j

[27] Ryckaert, J.P.; Ciccotti, G.; Berendsen, H.J. Numerical integration of the cartesian equations of motion of a system with constraints: molecular dynamics of n-alkanes. *Journal of Computational Physics,* 1977, 23, 327-341. Doi: 10.1016/0021-9991(77)90098-5

[28] Allen, M.P.; Tildesley, D.J. *Computer Simulation of Liquids.* Oxford, 1999, UK: Clarendon Press. Doi: 10.2307/2938686

[29] Frenkel, D.; Smit, B. *Understanding Molecular Simulation: From Algorithms to Applications.* 2002, San Diego, CA: Academic Press. Doi: 10.1063/1.881812

[30] Berendsen, H.J.C.; Postma, J.P.M.; van Gunsteren, W.F.; DiNola, A.; Haak, J.R. Molecular-Dynamics with Coupling to an External Bath. *Journal of Chemical Physics*, 1984, 81, 3684-3690. Doi: 10.1063/1.448118

[31] Duhovny, D.; Nussinov, R.; Wolfson, H.J. *Efficient unbound docking of rigid molecules*, 2002, 185-200, Berlin Heidelberg: *Springer-Verlag.* Doi: 10.1007/3-540-45784-4_14

[32] Zhang, C.; Vasmatzis, G.; Cornette, J.L.; DeLisi, C. Determination of atomic desolvation energies from the structures of crystallized proteins. *Journal of Molecular Biology*, 1997, 267, 707-726. Doi: 10.1006/jmbi.1996.0859

[33] Laskowski, R.A. PDBsum: summaries and analyses of PDB structures. *Nucleic Acids Research*, 2001, 29, 221-222. Doi: 10.1093/nar/29.1.221

[34] Daniel, R.R.; Thomas, E.C. III PTRAJ and CPPTRAJ: Software for Processing and Analysis of Molecular Dynamics Trajectory Data. *Journal of Chemical Theory and Computation*, 2013, 9, 3084-3095. Doi: 10.1021/ct400341p

[35] Pettersen, E.F.; Goddard, T.D.; Huang, C.C.; Couch, G.S.; Greenblatt, D.M.; Meng, E.C.; Ferrin, T.E. UCSF Chimera--a visualization system for exploratory research and analysis. *Journal of Computational Chemistry*, 2004, 25, 1605-1612. Doi: 10.1002/jcc.20084

[36] Humphrey, W.; Dalke, A.; Schulten, K. VMD: visual molecular dynamics. *Journal of Molecular Graphics*, 1996, 14, 33–38. Doi: 10.1016/0263-7855(96)00018-5

[37] *Krieger, E.; Koraimann, G.; Vriend, G.* Increasing the precision of comparative models with YASARA NOVA—a self-parameterizing force field. *Proteins, 2002, 47, 393-402.* Doi: 10.1002/prot.10104

[38] Andricioaei, I.; Karplus, M. On the calculation of entropy from covariance matrices of the atomic fluctuations. *J. Chem. Phys.*, 2001, 115, 6289. Doi: 10.1063/1.1401821

[39] Yoon, J.; Park, J.; Jang, S.; Lee, K.; Shin, S. Conformational characteristics of unstructured peptides: alpha-synuclein. *Journal of Biomolecular Structure and Dynamics*, 2008, 25, 505-515. Doi: 10.1080/07391102.2008.10507197

[40] Han, H.; Weinreb, P.H.; Lansbury, P.T. Jr The core Alzheimer's peptide NAC forms amyloid fibrils which seed and are seeded by β-amyloid: Is NAC a common trigger or target in neurodegenerative disease? *Journal of Chemistry & Biology*, 1995, 2, 163–169. Doi: 10.1016/1074-5521(95)90071-3

[41] *Kabsch, W.; Sander, C.* Dictionary of protein secondary structure: pattern recognition of hydrogen-bonded and geometrical features. *Biopolymers,* 1983, 22, 2577-2637. Doi: 10.1002/bip.360221211